Article

Chinese Science Bulletin

Condensed Matter Physics

June 2012 Vol.57 No.17: 2083–2086
doi: 10.1007/s11434-012-5175-2

Emission characteristics of surface second-order metal grating distributed feedback semiconductor lasers

SHI JunXiu[1,2], QIN Li[1*], LIU Yun[1], ZHANG Nan[1,2], ZHANG Jian[1,2], ZHANG LiSen[1,2], JIA Peng[1,2], NING YongQiang[1], ZENG YuGang[1], ZHANG JinLong[1] & WANG LiJun[1]

[1] *Key Laboratory of Excited State Processes, Changchun Institute of Optics, Fine Mechanics and Physics, Chinese Academy of Sciences, Changchun 130033, China;*
[2] *Graduate University of the Chinese Academy of Sciences, Beijing 100049, China*

Received October 26, 2011; accepted January 16, 2012

To obtain high-power semiconductor lasers with stable operation in a single longitudinal mode and improve the characteristics of the output beam, an end-emitting surface second-order metal grating distributed feedback (DFB) laser emitting at around 940 nm is fabricated. The characteristics of the uncoated devices with and without gratings are tested under room temperature continuous-wave conditions without any temperature-control device and compared. The devices with gratings achieve high powers of up to 385 mW/facet and a small lateral far-field angle of 2.7° at 1.5 A, have only 4.13 nm/A wavelength-shift, and 0.09 nm spectral linewidth at 600 mA, and operate in a stable longitudinal mode. Devices without gratings operate in multimode, with a larger lateral far-field angle (7.3°) and spectral linewidth (1.3 nm), although with higher output powers. Because of the integration of second-order metal gratings and their very high coupling capability, the output beam quality is improved greatly, the lasing wavelength is stable and varies slowly with changes in injection current, while the spectrum is narrowed dramatically, and the far-field angles are greatly reduced. This opens the way for the realization of watt-scale power broad-stripe (>100 μm) surface second-order metal grating end and surface-emitting DFB lasers and arrays with single frequency, single mode operation and high output beam quality.

broad-stripe DFB laser, surface second-order metal grating, holographic photolithography

Citation: Shi J X, Qin L, Liu Y, et al. Emission characteristics of surface second-order metal grating distributed feedback semiconductor lasers. Chin Sci Bull, 2012, 57: 2083–2086, doi: 10.1007/s11434-012-5175-2

High power broad-stripe lasers are widely used as pump sources for solid-state lasers, fiber lasers and fiber amplifiers. In particular, lasers emitting at 940 nm are widely used to pump Yb^{3+}:YAG solid-state lasers, and Yb-doped fiber lasers and fiber amplifiers, which require high power, a stable lasing frequency, small far field angles and narrow spectral linewidth. However, conventional broad-stripe lasers have clear deficiencies in their performance, because of a spectral linewidth of 2–4 nm, a wavelength shift with temperature of approximately 0.3 nm/K and large wavelength changes with increasing current and aging time [1]. Also, the overall beam quality is poor. These deficiencies limit the direct applications of high power broad stripe lasers. Several approaches have been used to stabilize the emission wavelength, narrow the spectrum and improve the output beam quality of these pump lasers, all of which were based on establishing spectrally selective feedback, such as the combination of an external collimation lens and a volume Bragg grating (VBG) [2–4], external fiber Bragg gratings (FBG) [5–10] and distributed feedback gratings integrated into the laser chip (DFB laser) [11–13]. However, the requirement for a collimating lens and alignment of the VBG and FBG makes both of these approaches complex and expensive. Diode lasers with internal Bragg gratings need no other expensive parts or external adjustment and have the advantages of a dynamic single mode, compact size, and integration

*Corresponding author (email: qinl@ciomp.ac.cn)

capability [11–13], which makes broad-stripe DFB lasers potentially attractive. In this paper, broad-stripe DFB lasers with large-area surface second-order metal gratings are proposed. Second-order DFB lasers can eliminate the degenerate modes of conventional first-order DFB lasers, achieve single mode operation and improve the beam quality, depending on the two diffraction orders of the second-order grating. Surface metal gratings, when compared to dielectric gratings, have the advantages of grating fabrication without epitaxial re-growth and thermal impedance minimization. The method used in this paper can also achieve batch production.

In this paper, we fabricated the end-emitting lasers with surface second-order metal gratings and without gratings, both emitting at around 940 nm, using holographic photolithography and wet etching technologies, and compared the emission characteristics of the devices after experimental testing under continuous wave and room temperature conditions and without any temperature control device.

1 Device structure and fabrication

The wafer structure for fabrication of the 940 nm DFB lasers with surface second-order metal gratings is a traditional edge-emitting semiconductor laser structure and is composed of eight layers: a 200 nm GaAs cap layer, a 50 nm $GaIn_{0.49}P$ smoothing layer, a 1 μm p-$Al_{0.2}GaIn_{0.49}P$ cladding layer, a 0.4 μm p-$GaIn_{0.49}P$ guiding layer, a 19 nm $GaIn_{0.11}As$ active layer, a 0.4 μm n-$GaIn_{0.49}P$ guiding layer, a 1 μm n-$Al_{0.2}GaIn_{0.49}P$ cladding layer, and the n-GaAs substrate layer.

The schematic diagram of the 940 nm surface second-order metal grating DFB laser is shown in Figure 1. We fabricated end-emitting lasers with surface second-order metal gratings and without these gratings. For an emitting wavelength of 940 nm and large area (960 μm×142 μm) gratings, the period of the first-order grating exceeds the diffraction limit of the holographic light, so holographic methods cannot be used, and using electron beam direct writing to fabricate large-area gratings needs several splices and would introduce uncontrollable stitching errors. We therefore used holographic photolithography to fabricate large area (960 μm×142 μm) second-order gratings.

The fabrication processes were as follows. First, a 200 nm-thick SiO_2 film was deposited on the cap layer. Then, a stripe groove (960 μm×142 μm×950 nm) was obtained by photolithography and wet chemical etching, with 200 nm SiO_2, 200 nm GaAs, 50 nm $GaIn_{0.49}P$ and 500 nm $Al_{0.2}GaIn_{0.49}P$ layers etched in turn. Then, the holographic exposure and wet etching methods were used to fabricate second-order gratings in the stripe groove, with grating area of 960 μm× 142 μm, grating period Λ=287 nm, grating depth d_g=70 nm, and grating duty cycle $\sigma=b/\Lambda$=0.35. After fabrication of the gratings, AuGeNi was deposited on the n-side and annealed

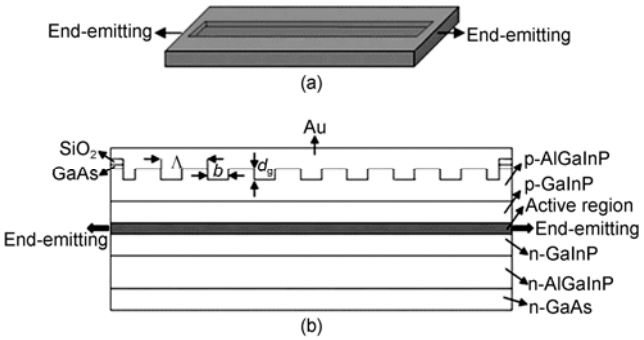

Figure 1 (a) Schematic representation of the surface second-order metal grating DFB laser with 1 mm cavity length, and 142 μm wide ohmic contact groove; (b) schematic cross-section of the laser.

at 400°C. Then, 20 nm Ti/20 nm Pt/200 nm Au layers were deposited on the p-side to form the Au/$Al_{0.2}GaIn_{0.49}P$ gratings and also pattern the p-contacts, but without annealing to ensure a large index difference at the metal/semiconductor interface. Devices were fabricated both with the Bragg gratings and without gratings, and the total cavity length was L=1 mm, so that the only fabrication difference between the two types of devices is the presence or lack of a grating structure.

Figure 2(a) shows the scanning electron microscopy (SEM) image of the grating profile, and Figure 2(b) shows the three-dimensional atomic force microscopy (AFM) graph. The grating period is 287 nm, and the grating depth is 70 nm. The profile shape lies in an area between trapezoidal and sinusoidal. The distribution of the grating fringes is very uniform, and the grating morphology is clear. The gratings are located at the metal/semiconductor interface in the p-$Al_{0.2}GaIn_{0.49}P$ cladding layer. A large built-in index difference exists at this interface, which can provide a high

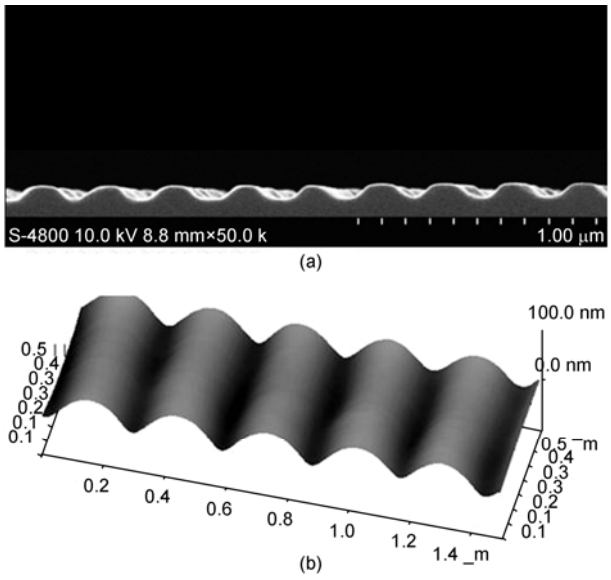

Figure 2 (a) SEM image of the grating profile after wet chemical etching; (b) three-dimensional AFM morphology of the grating profile.

coupling capability and control the optical mode and stability [13] to obtain the laser output with a single frequency and a single mode.

2 Results and discussion

The end-emitting characteristics of the uncoated lasers with surface second-order metal gratings and those without gratings were tested under continuous wave (CW) and room temperature conditions without any temperature control device, and the results were compared. The surface-emitting characteristics of the DFB laser are not measured, because the first-order diffraction of the second-order gratings, which causes the 90° radiation losses and provides the surface-emitting laser output, is lost as dissipation in the metal, and there is no window for surface emission. The experimental results are shown in Figures 3 and 4.

Figure 3(a) shows the CW light-current, *I-V* and far-field profiles of the DFB laser with the surface second-order metal gratings at a current of 1.5 A. The threshold current is 0.32 A, and the slope efficiency is 0.4 W/A. The optical

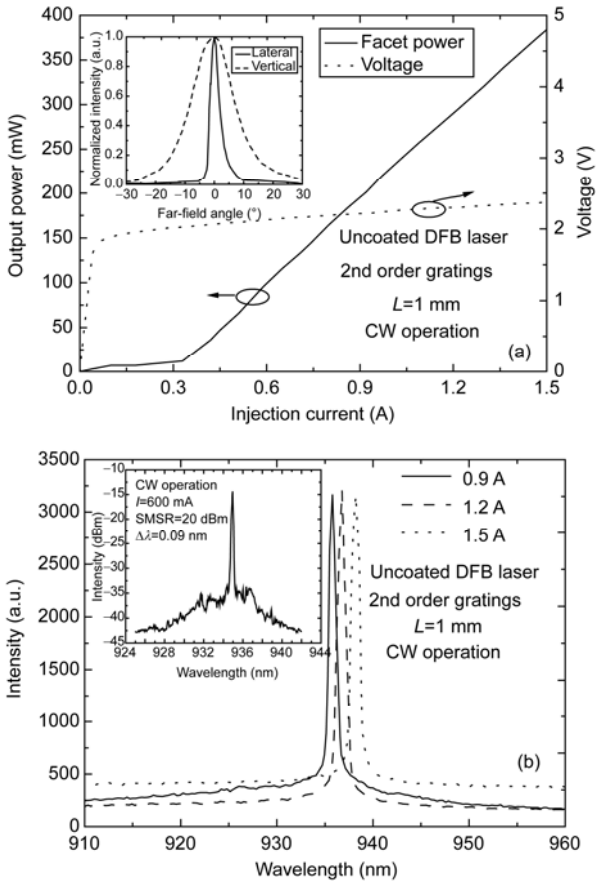

Figure 3 (a) CW light-current and *I-V* characteristics. Inset: normalized far-field profiles at a current of 1.5 A. (b) Emission spectrum measured at different currents for DFB laser with surface second-order metal gratings at room temperature. Inset: spectrum measured at 600 mA using Ando AQ6315B Spectral Analyzer.

power is as high as 385 mW/facet, the lateral far-field angle (FWHM) is less than 2.7° and the vertical far-field angle (FWHM) is only 16.7°. Both far-field angles are small, because the second-order metal gratings limit the operation of the modes to confine and outcouple the output beam over the emitting aperture. Figure 3(b) shows the emission spectrum measured from 0.9 to 1.5 A with steps of 0.3 A using an USB2000+VIS-NIR spectrometers from Ocean Optics with 0.35 nm resolution. The spectral linewidth (FWHM) is less than 0.5 nm at a current of 1.5 A, and the maximum central-wavelength shift with current is only 4.13 nm/A from 0.9 to 1.5 A. The spectrum measured at a current of 600 mA using an Ando AQ6315B spectral analyzer and a 6 μm core diameter fiber with 0.02 nm resolution shows that the DFB laser operates in a single longitudinal mode, the side mode suppression ratio (SMSR) is 20 dBm, and the spectral linewidth is 0.09 nm. The second-order grating plays a triple role, providing feedback, outcoupling and mode selection. Because of their high coupling capability, the contribution of the surface second-order metal gratings to obtaining high-power semiconductor lasers with stable operation in a single longitudinal mode and to improving the characteristics of the output beam are very prominent.

Figure 4(a) shows the CW light-current, *I-V* and far-field profiles of the laser without gratings at a current of 1.5 A. Both devices show large ohmic resistance of 0.23 Ω, because of the low doping of the p-cladding layer replacing the cap layer as the contact layer, and the surface oxidation of Al also leads to a high resistance. The optical power is nearly 600 mW larger than that of the DFB lasers, but the lateral far-field angle is 7.3° and the vertical far-field angle is 36°, which are both worse than for the DFB lasers. Figure 4(b) shows the emission spectrum from 1 to 2 A with steps of 0.5 A. The laser without gratings operates in multimode, the spectral linewidth is 1.3 nm at a current of 1.5 A, and the central wavelength shifts with current for the fundamental mode and the higher order mode are 14.72 and 19.52 nm/A, respectively. As discussed above, the advantages of the DFB lasers are highly significant.

3 Conclusions

In conclusion, we have produced a 940 nm broad-stripe surface second-order metal grating DFB laser with up to 385 mW CW output power, a 2.7° small lateral far-field angle, 0.09 nm spectral linewidth, and operating in a stable single longitudinal mode. Because of the integration of the second-order metal grating and its very high coupling capability, the output beam quality is improved greatly; the lasing wavelength is stable and varies slowly when the injection current changes, the spectrum is narrowed dramatically, and the far-field angles are greatly reduced. This opens the way for the realization of watt-scale high-power broad-stripe (>100 μm) surface second-order metal grating end and surface-

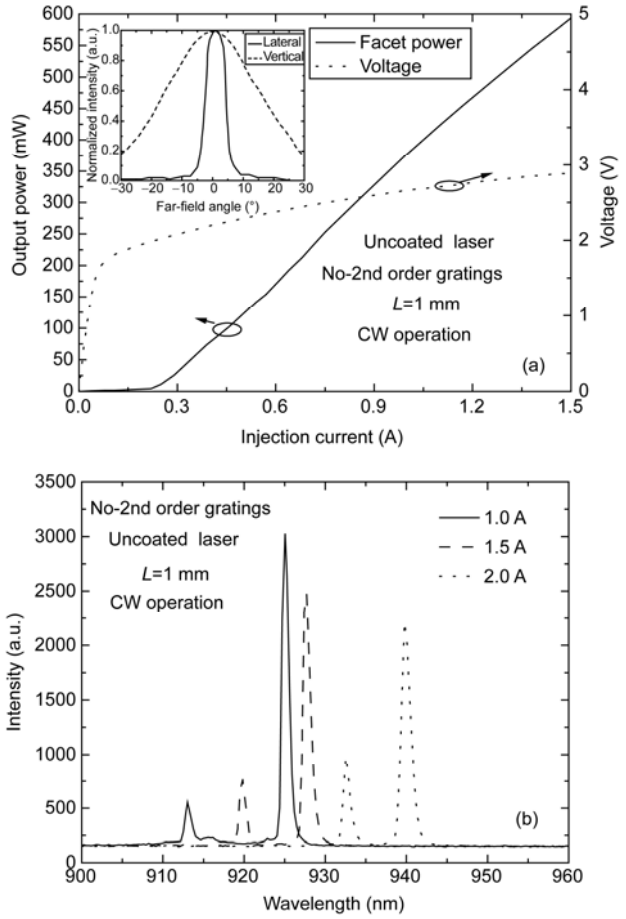

Figure 4 (a) CW light-current and *I-V* characteristics. Inset: normalized far-field profiles at a current of 1.5 A. (b) Emission spectrum measured at different currents for laser without gratings at room temperature.

emitting DFB lasers and arrays with single frequency, single mode operation and high output beam quality.

This work was supported by the National Natural Science Foundation of China (90923037, 61106068 and 61176045). The authors are also grateful to Jin Yu from the College of Electronic Science and Engineering, Jilin University for providing holographic photolithography assistance.

1 Klehr A, Bugge F, Erbert G, et al. High power broad area 808 nm DFB lasers for pumping solid state lasers. Proc SPIE, 2006, 6133: 61330F
2 Venus G B, Sevian A, Smirnov V I, et al. High brightness narrow-line laser diode source with volume Bragg grating feedback. Proc SPIE, 2005, 5711: 166–176
3 Rudder S L, Connolly J C, Steckman G J. Hybrid ECL/DBR wavelength and spectrum stabilized lasers demonstrate high power and narrow spectral linewidth. Proc SPIE, 2006, 6101: 61010I
4 Schnitzler C, Hambuecker S, Ruebenach O, et al. Wavelength stabilization of HPDL array-fast-axis collimation optic with integrated VHG. Proc SPIE, 2007, 6456: 645612
5 Toshiya S. Design of a fiber Bragg grating external cavity diode laser to realize mode-hop isolation. IEEE J Quant Electron, 2007, 43: 838–845
6 Long P, Carignan J. Sliced fiber Bragg grating used as a laser diode external cavity. Proc SPIE, 2009, 7386: 73862S
7 Juodawlkis P W, O'Donnell F J, Brattain M A, et al. High-power, ultra-noise semiconductor external cavity lasers based on low-confinement optical waveguide gain media. Proc SPIE, 2010, 7616: 76160X
8 Hashimoto J I, Takagi T, Kato T, et al. Fiber-Bragg-grating external cavity semiconductor laser (FGL) module for DWDM transmission. J Lightwave Technol, 2003, 21: 2002–2009
9 Yu H G, Wang Y, Xu Q Y, et al. Characteristics of multimode fiber Bragg gratings and their influences on external-cavity semiconductor lasers. J Lightwave Technol, 2006, 24: 1903–1912
10 Mikel B, Helan R, Cip O, et al. Stabilization of semiconductor lasers by fiber Bragg gratings. Proc SPIE, 2008, 7155: 71552T
11 Crump P, Schultz C M, Pietrzak A, et al. 975-nm high-power broad area diode lasers optimized for narrow spectral linewidth applications. Proc SPIE, 2010, 7583: 75830N
12 Klehr A, Wenzel H, Brox O, et al. High-power 894 nm monolithic distributed-feedback laser. Opt Exp, 2007, 15: 11364–11369
13 Li S, Witjaksomo G, Macomber S, et al. Analysis of surface-emitting second-order distributed feedback lasers with central grating phaseshift. IEEE J Sel Topics Quant Electron, 2003, 9: 1153–1165